RSC Advances

COMMUNICATION

View Article Online
View Journal | View Issue

Cite this: *RSC Adv.*, 2014, **4**, 4122

Received 13th August 2013
Accepted 20th November 2013

DOI: 10.1039/c3ra46602g

www.rsc.org/advances

Aminoclay-templated nanoscale zero-valent iron (nZVI) synthesis for efficient harvesting of oleaginous microalga, *Chlorella* sp. KR-1†

Young-Chul Lee,‡[ae] Kyubock Lee,‡[b] Yuhoon Hwang,[c] Henrik Rasmus Andersen,[c] Bohwa Kim,[b] So Yeun Lee,[b] Moon-Hee Choi,[d] Ji-Yeon Park,[b] Young-Kyu Han,[f] You-Kwan Oh*[b] and Yun Suk Huh*[a]

Synthesis of aminoclay-templated nanoscale zero-valent iron (nZVI) for efficient harvesting of oleaginous microalgae was demonstrated. According to various aminoclay loadings (0, 0.25, 0.5, 1.0, 2.5, 5.0, and 7.5 aminoclay–nZVI ratios), the stability of nZVI was investigated as a function of sedimentation rate. Aminoclay-coated nZVI (aminoclay–nZVI composites) showed optimal dispersibility at the 1.0 ratio, resulting in the smallest aggregated size and uniform coating of aminoclay nanoparticles onto nZVI due to electrostatic attraction between nZVI and aminoclay nanoparticles. This silica-coated nZVI composite (ratio 1.0) exhibited a highly positively charged surface (~+40 mV) and a ferromagnetic property (~30 emu g^{-1}). On the basis of these characteristics, oleaginous *Chlorella* sp. KR-1 was harvested within 3 min at $a > 20$ g L^{-1} loading under a magnetic field. In a scaled-up (24 L) microalga harvesting process using magnetic rods, microalgae were successfully collected by attachment to the magnetic rods or by precipitation. It is believed that this approach, thanks to the recyclability of aminoclay–nZVI composites, can be applied in a continuous harvesting mode.

Introduction

Over the past few decades, microalgae biomass as a third-generation energy source has been intensively explored both theoretically and for industrial applications to sustain biodiesel production.[1–3] Thanks to its utilization of barren lands and non-grain feedstocks, microalgae-based biorefinement is a promising alternative source of transportation fuels.[4,5] However, challenges presented by the limitations of the relevant biorefinement processes have to be overcome before microalgae can be considered as a feedstock.[6,7]

Microalgae-based biorefinement entails several downstream processes including cultivation, harvesting, dewatering, and extraction of invaluable products such as proteins, carbohydrates, and lipids.[8–10] Biorefinement's commercialization requires that all of these processes be developed for significantly improved cost-efficiency. Indeed, many researchers have devoted themselves to the study and improvement of these processes. Conventional centrifugation, flocculation by organic/inorganic coagulants, precipitation by pH increment, filtration including membrane processes, and flotation have all been investigated and reported on for harvesting purposes.[7] Recently too, the use of magnetic nanoparticles (Fe_3O_4), owing to the fast harvesting and easy recovery thus achievable, has become an issue.[11,12] However, the use of magnetic nanoparticles for microalgae harvest is depending on specific pH range at which zeta potential of magnetic nanoparticles shows positively charged surface. As a result, the coating of cationic charged materials onto magnetic particles is demanding.[13]

Since 1997, organophyllosilicates consisting of organic functional groups such as amino, thiol, phenol, hydroxyl, and others as well as backboned cationic metals by sol–gel reaction under ambient conditions have been reported.[14–16] Among them, 3-aminopropyl-functionalized magnesium phyllosilicate (denoted as aminoclay) has been widely used in the fabrication of bio(nano)composites[17–20] and environmental clean-ups,[21–24] which are associated to specifically *via* a process of self-assembly due to the protonation of amine groups and the

[a]*Department of Biological Engineering, College of Engineering, Inha University, Incheon 402-751, Republic of Korea. E-mail: yunsuk.huh@inha.ac.kr; Fax: +82-42-865-3613; Tel: +82-42-865-3610*

[b]*Clean Fuel Department, Korea Institute of Energy Research, 152 Gajeong-ro, Yuseong-gu, Daejeon 305-343, Republic of Korea. E-mail: ykoh@kier.re.kr; Fax: +82-42-860-3495; Tel: +82-42-860-3697*

[c]*Department of Environmental Engineering, Technical University of Denmark, Bygningstorvet, Building 115, 2800 Kgs. Lyngby, Denmark*

[d]*Department of Beauty and Cosmetology, Graduate School of Industry, Chosun University, Gwangju 501-759, Republic of Korea*

[e]*Department of Civil and Environmental Engineering (BK21 program), KAIST, 291 Daehakno, Yuseong-gu, Daejeon 305-701, Republic of Korea*

[f]*Department of Energy and Materials Engineering, Dongguk University-Seoul, Seoul 100-715, Republic of Korea*

† Electronic supplementary information (ESI) available. See DOI: 10.1039/c3ra46602g

‡ These authors equally contributed to this work. Y.-C. L. and Y.-K. O. conceived the research idea; Y.-C. L., K. L., Y. H., B. K. and S. Y. L. performed the experiments; Y.-C. L., K. L., Y. H., H. R. A., M.-H. C., J.-Y. P., Y.-K. H., Y.-K. O. and Y. S. H. analyzed the results; Y.-C. L., K. L., Y.-K. O. and Y. S. H. wrote the paper.

delamination of aminoclay sheets in aqueous solution. Very recently, Lee *et al.* has intensively studied the destabilization of various cells by antibacterial assays,[25] harmful algal lysis,[26] and oleaginous microalgae harvesting.[27–29] In this harvesting application, the recovery and recycling of aminoclay represent major challenges.

One approach to overcoming this limitation is to coat aminoclay onto magnetic nanoparticles (nanoscale zero-valet iron (nZVI) or magnetite (Fe_3O_4)) for improved recovery efficiency. nZVI usually is synthesized by reduction of Fe^{2+} or Fe^{3+} ions with reducing agents (which are applied within the field of environmental sciences both as reduction and oxidation agents.[30,31]) Specifically, nZVI is synthesized by solution chemistry in the presence of aminoclay (<50 nm average hydrodynamic diameter) as a template,[32] as an immediate consequence of which, organo-building blocks of aminoclay coat nZVI nanoparticles. In these pages the focus is on nZVI synthesis rather than Fe_3O_4, due its stronger magnetic property and larger size for facile aminoclay coating.[33]

In this context, the present study investigated simple synthesis of aminoclay-coated nZVI for efficient harvesting of an oleaginous microalga, *Chlorella* sp. KR-1. Harvesting in a batch mode was successfully completed within 3 min. Moreover, a scaled-up (24 L) process for the purpose of continuous harvesting was successfully achieved, which also reduced the aminoclay loading. Thus, this aminoclay-coated-nZVI harvesting approach might represent a promising candidate as a downstream process for microalgae feedstocks in the biorefinement context.

Experimental methods

Preparation of aminoclay and aminoclay–nZVI composites

Aminoclay was synthesized according to the procedures documented in the literature.[10,25–28] Briefly, 8.4 g (~0.04 mol) of $MgCl_2 \cdot 6H_2O$ (Junsei, Japan) was added to 200 mL of ethanol solution (95%) obtained from Samchun Pure Chemicals (Pyungtack, Korea). After fully dissolving the $MgCl_2 \cdot 6H_2O$ in ethanol solution by 10 min stirring, 13 mL (~0.06 mo1) of 3-aminopropyltriethoxysilane (Sigma-Aldrich, USA) was added drop-wise to the ethanolic solution containing magnesium chloride. The mixture was stirred overnight. The white precipitate (*i.e.*, aminoclay) was centrifuged (3000× *g*, 10 min) and subsequently harvested. The products were then oven-dried at 50 °C overnight.

In a typical precipitation method,[34] after preparation of 4 g aminoclay solution in 50 mL distilled water, 1.9 g $FeCl_3 \cdot 6H_2O$ and 0.7 g $FeCl_2 \cdot 4H_2O$ were dissolved with stirring. To above mixture, 30 mL of 1.0 M NaOH was added rapidly with vigorous stirring. And then centrifugation (6000 rpm for 10 min) was collected with the aminoclay–Fe_3O_4 composite.

Synthesis of the aminoclay–nZVI composites[35] (*i.e.*, aminoclay-coated nZVI) was performed as noted below. First, the desired amount of aminoclay was solubilized in 100 mL of double-distilled water preparatory to 10 min sonication in a 250 mL beaker, to which was introduced 50 mL of a ferric (Fe^{3+}) solution (35.8 mM, $FeCl_3 \cdot 6H_2O$, Sigma-Aldrich, USA). Then, 50 mL of sodium borohydride solution (179 mM, Sigma-Aldrich, USA) was introduced into the beaker drop-wise and vigorously mixed for 25 min, thereby reducing the ferric ions to nZVI. The concentrations of solutions were determined based on eqn (1) and the conditions indicated in Table 1. The aminoclay–nZVI composite slurry was aged under the anoxic conditions for 1 day for full coating of nZVI and the resultant reduction of H_2 gas generation. After two-times washing with N_2-gas-purged double-distilled water, the aminoclay–nZVI composite slurry was ready for further microalgae harvesting.

$$4Fe^{3+} + 3BH_4^- + 9H_2O \rightarrow 4\ Fe^0 + 3H_2BO_3^- + 12H^+ + 6H_2 \quad (1)$$

Chlorella sp. KR-1 strain and growth conditions

The oleaginous freshwater microalgal species employed in this study was *Chlorella* sp. KR-1,[27,28] as cultured in a nutrient media at pH 6.5 (media constituents: KNO_3, 3 mM; KH_2PO_4, 5.44 mM; Na_2HPO_4, 1.83 mM; $MgSO_4 \cdot 7H_2O$, 0.20 mM; $CaCl_2$, 0.12 mM; FeNaEDTA, 0.03 mM; $ZnSO_4 \cdot 7H_2O$, 0.01 mM; $MnCl_2 \cdot 4H_2O$, 0.07 mM; $CuSO_4$, 0.07 mM; $Al_2(SO_4)_3 \cdot 18H_2O$, 0.01 mM). It had been cultivated at 30 °C in a Pyrex bubble-column reactor (working volume: 6 L) equipped with 12 fluorescent lamps at the front and right/left sides (light intensity: 80 μmol m^{-2} s) in a constant-temperature room at 30 °C for 7 days. It was supplied with 10% (v/v) CO_2 in air at a rate of 0.75 L min^{-1}. The oil content of *Chlorella* sp. KR-1 is 36.5–41.0% (weight of oil/dried biomass).

Microalgae harvesting process

Microalgae solution of 1.5 g L^{-1} microalgae concentration was removed from the 6 L scaled bubble-column reactor. For the purposes of batch-scale microalgae harvesting, the aminoclay–nZVI composites were mixed in a 6 mL microalgal solution in a 15 mL test tube. After vigorous mixing for 1 min, multiple test tubes containing various dosages of aminoclay–nZVI composites were left on magnetic ferrite bricks (surface magnetic-field strength: 1570 G). The supernatant was obtained for optical density (OD) measurement at the 680 nm wavelength for 3 and 30 min at the 2/3 height from the vial bottom using a UV-visible spectrophotometer (UV-1800, Shimadzu, Japan). The harvesting efficiency (%) was determined by equation eqn (2),

$$\text{Efficiency}(\%) = \left[1 - \frac{OD_f}{OD_i}\right] \times 100, \quad (2)$$

where OD_f and OD_i are the final and initial OD values of the culture media, respectively. All of the experiments were conducted in duplicate, and the values were averaged.

For a 24 L-scale demonstration, appropriate amounts of the aminoclay–nZVI composites were directly added to a designed

Table 1 Conditions for aminoclay-templated nZVI synthesis in aqueous solution

Fe^{3+} concentration (g L^{-1})	0.5 g L^{-1}						
$[Fe^{3+}] : [BH_4^-]$	1:5 (35.8 mM Fe^{3+} : 179 mM BH_4^-)						
[Aminoclay] : $[Fe^{3+}]$	0	0.25	0.5	1.0	2.5	5.0	7.5

reactor containing 24 L of microalgal solution. To make homogenous mixtures, air-bubbling by means of a metal membrane sparger was maintained for several minutes, after which 5 magnetic rods (surface magnetic-field strength: 9200 G; diameter: 22 mm; length: 500 mm) were applied for magnetophoretic separation by microalgae flocculated with aminoclay–nZVI composites.

Sample characterization and instruments

Bare nZVI and the aminoclay–nZVI composites were analyzed under transmission electron microscopy (TEM, JEM-2100F) on 300-mesh carbon-coated copper grids. Photographic images were all captured with an iPhone 5 digital camera. Powder X-ray diffraction (XRD) patterns were assessed by D/MAX-RB (Rigaku, 12 kW) after drying (by removal of water using filter papers and tissues and by subsequent milling). The Fourier transform infrared (FT-IR) spectra (FTIR 4100) of KBr pellets composed of 10 wt% vacuum-dried targeting sample and 90 wt% KBr powder were recorded within the 4000 cm^{-1}–400 cm^{-1} range. Zeta-potential measurements were obtained with a Zetasizer Nano-ZS particle analyzer (Zetasizer nano zs, Malvern, UK). Magnetic measurements of the powdered samples were carried out using a model 4HF vibrating-sample magnetometer (VSM, ADE Co. Ltd, USA) with a maximum magnetic field of 20 kOe. A quantitative analysis of the aminoclay and nZVI was performed with silicon and total ionic iron by 5 mL of 10 mM HCl in aqueous solution after 10 min standing by inductively coupled plasma atomic emission spectrometry (ICP-AES, Optima 7300 DV, each calibration curve in ESI, Fig. S1†). The morphologies of the microalgae and harvested microalgae were examined under bright optical microscopy (Axio Imager A2, Carl Zeiss Microscopy GmbH, Jena, Germany) in the fluorescence mode. Also, scanning electron microscopic (SEM) images were obtained following the manufacturer's bio-sample preparation protocol. The pH variation was monitored using a pH/ion meter (D-53, Horiba).

Results and discussion

Characteristics of aminoclay–nZVI composites

The as-prepared aminoclay was composed of a cationic metal center (Mg^{2+}) with sandwiching of $-(CH_2)_3NH_2$ organofunctional pendents *via* covalent bonding, as shown in its approximate unit structure in ESI, Fig. S2†.[10] In a proton-rich aqueous solution the amine groups' high-nitrogen density was protonated to yield cationic charged clusters. For delaminated aminoclay nanoparticle (<50 nm)-coated nZVI surfaces, the growth of the nZVI nanoparticles was stable, which is to say, well-dispersible in aqueous solution, due to the electrostatic repulsion by aminoclay nanoparticles.

Sedimentation profiles of the synthesized aminoclay–nZVI composites with different aminoclay loadings were obtained by spectrophotometry. Inferences on the sedimentation behavior were evaluated based on the evolutionary characteristics of the suspensions' optical absorbances over time. The normalized absorbances of the suspensions with different amounts of aminoclay are plotted in Fig. 1(a) as functions of time. nZVI

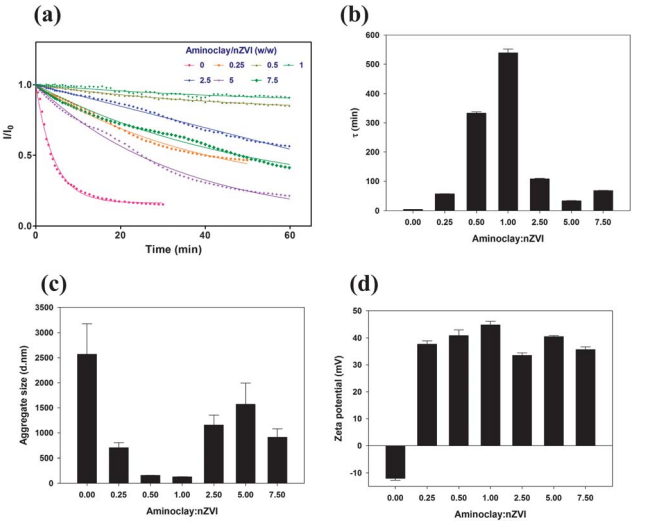

Fig. 1 (a) Sedimentation test as function of time, (b) sedimentation parameter (τ) from eqn (3), (c) aggregate sizes and (d) zeta potential values of bare nZVI and aminoclay–nZVI composites (0.25, 0.5, 1.0, 2.5, 5.0, and 7.5 weight ratio).

nanoparticles, due to their large density and diameter, settle down; consequently, the general tendency of the normalized absorbance is to decrease with time. The sedimentation patterns could be interpreted by the equation[36–38]

$$I_t = I_0 e^{-t/\tau}, \quad (3)$$

where I_t is the absorbance of the solution at time t, I_0 is the initial absorbance, and τ is the characteristic time related to the hydrodynamic radius of the particles.

As illustrated in Fig. 1(a), the sedimentation profile was significantly affected by the aminoclay–Fe weight ratio. With the increase in the aminoclay loading upto 1.0, the stability was significantly increased. However, at ratios higher than 2.5, sedimentation was accelerated, which fast sedimentation might be due to the significant flocculation phenomena. The characteristic time, τ, as calculated from the sedimentation profile, is presented in Fig. 1(b). According to the sedimentation profiles, the characteristic time varied from 4.30 to 539 min, and the aminoclay–nZVI composite showed the most stable colloidal behaviors at the 1.0 ratio.

It is fitting that the aggregated size (diameter, nm) as measured by dynamic light scattering was the smallest, 130 nm, at the aminoclay–nZVI composite ratio of 1.0 (Fig. 1c). At that time, the slurry of the aminoclay–nZVI composites changed to a highly positively charged surface: from −12 mV in the absence of aminoclay to ~+40 mV after aminoclay coating (Fig. 1e).

The morphological alternations of the aminoclay–nZVI composites also were examined (Fig. 2). Bare nZVI normally synthesizes chain-like spheres due to magnetic interaction and the core–shell structure of thin-shell iron oxides (γ-Fe_2O_3/Fe_3O_4) in Fe(0) (Fig. 2a and b).[39,40] In the presence of aminoclay however, the nZVI surface, in the present results, was uniformly coated with aminoclay (Fig. 2c–f); this result corresponded with the elemental mapping data (see ESI, Fig. S3†), indicating that

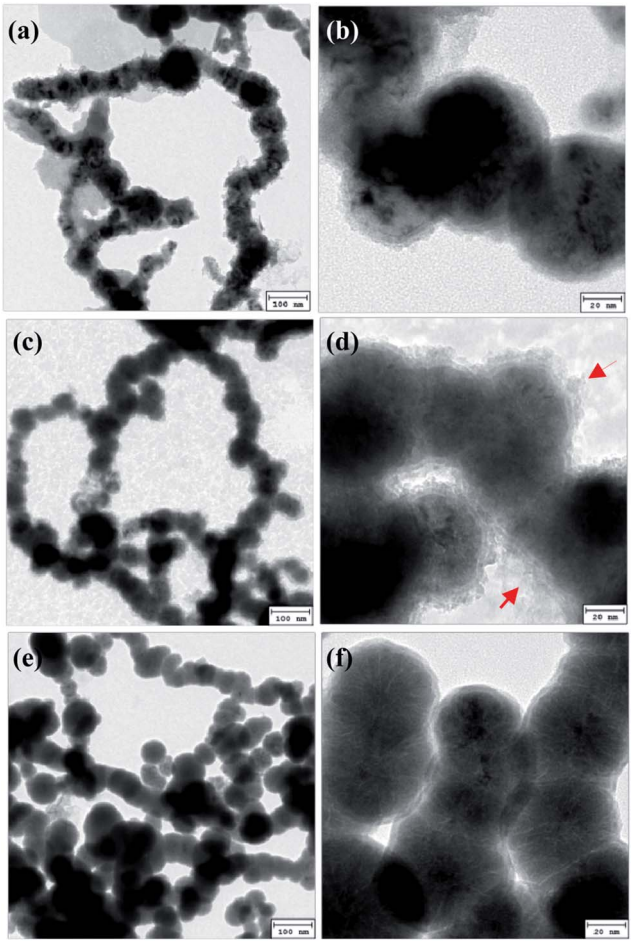

Fig. 2 Transmission electron microscopic (TEM) images of bare nZVI (0) (a and b), aminoclay–nZVI composite (0.25) (c and d), and aminoclay–nZVI composite (1.0) (e and f). The brown arrows in (d) indicate aminoclay nanoparticles.

Fe is from nZVI, Mg and Si represent the presence of aminoclay, and O and Cl are from both nZVI and aminoclay. Accordingly, the silica-coated nZVI hybrids became disconnected as the aminoclay loading increased (see ESI, Fig. S4†). At the higher aminoclay concentrations, linking of the nZVI nanoparticles was prevented by the steric effect, and significant flocculations occurred along with a significant increase of coating thickness, leading to increased sedimentation.

After 1 week's aging (*i.e.*, as stored in aminoclay solution; see ESI, Fig. S5†), the microalgal morphology was changed to a more chestnut-like shape where nZVI was oxidized, but the aminoclay coating was retained. Notably, in the case of co-precipitation of Fe_3O_4 synthesis in the presence of aminoclay (see ESI, Fig. S6†), the aminoclay coating was not inconsistent, owing to the smaller Fe_3O_4 size (<10 nm), which might be not suitable for aminoclay-particle coating. A larger size of Fe_3O_4 for aminoclay-coating applications, then, is recommended.

The X-ray diffraction (XRD) patterns of the crystalline structures of the aminoclay, bare nZVI, and aminoclay–nZVI composites were recorded (Fig. 3). Aminoclay showed basal spacing at d_{001} = 1.40 nm (2θ = 6.3°) and broad in-plane

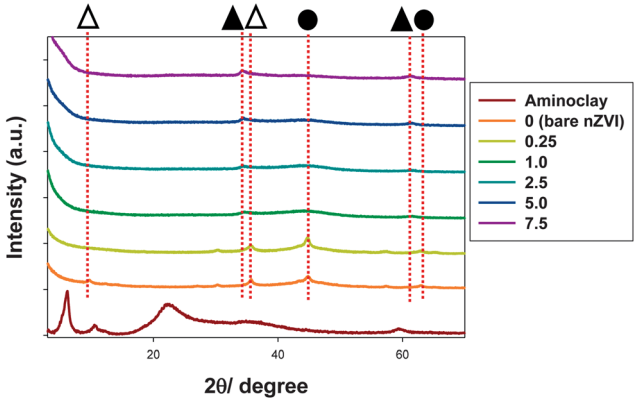

Fig. 3 Powder X-ray diffraction (XRD) patterns of aminoclay, bare nZVI, and aminoclay–nZVI composites with different weight ratios (0.25–7.5). The filled circles, the filled triangle and the empty triangle indicate standard cubic Fe(0), maghemite (γ-Fe_2O_3), and magnetite (Fe_3O_4), respectively.

reflections at $d_{020,110}$ = 0.39 nm (2θ = 22.9°), $d_{130,200}$ = 0.26 nm (2θ = 34.8°), and $d_{060,330}$ = 0.16 nm (2θ = 59.4°), indicating the presence of 2 : 1 trioctahedral smectite, one of the phyllosilicates. The basal spacing at d_{001} exhibited a regular layered-structure thickness characteristic of talc-like phyllosilicate, in agreement with the literature.[10,25–28]

In case of bare nZVI synthesis (ratio 0), iron oxide (maghemite (γ-Fe_2O_3), JCPDS no. 39-1346) and Fe(0) peaks appeared, which determined the core–shell structure that emerged in TEM images (Fig. 2a and b). With increased aminoclay loadings, peaks of mixed iron oxides (maghemite (γ-Fe_2O_3), JCPDS no. 39-1346 and magnetite (Fe_3O_4), JCPDS 19-0629)[39] and Fe(0) appeared, with no enhancement of the Fe(0) crystallinity. After 1 week's aging of the aminoclay–nZVI composite (ratio 1.0) by standing samples with open capping (see ESI, Fig. S7†), the intensity of the iron oxides' peaks was increased, but that of the standard cubic Fe(0) was maintained.[40,41] Thus, the morphological changes by nZVI oxidation and the crystalline structure showed a consistent trend, along with the retainment of magnetic property for recycle.

For their magnetic properties (see ESI, Fig. S8†), the nonlinear hysteresis loops with nonzero remnant magnetization (M_r) and coercivity (H_c) exhibited ferromagnetic properties like iron oxide core–shell structures.[42] The M_s values of nZVI and aminoclay–nZVI (ratio 1.0) showed ~100 and ~35 emu g^{-1}, respectively. The M_s value was reduced about 3-fold by aminoclay coating. This was owed to the organofunctional pendents in aminoclay.[43]

Batch-mode microalgae harvesting by aminoclay–nZVI composites

Based on the stability results of aminoclay–nZVI composites, the 1.0 ratio was selected as optimal for microalgae harvesting. Therefore, this highly positively charged composite was tested on a laboratory scale (10 mL vials) with oleaginous *Chlorella* sp. KR-1 according to loading amount under an external magnetic field. At > 20 g L^{-1} of aminoclay–nZVI composite, the microalgae was precipitated within 3 min (Fig. 4a and b and ESI,

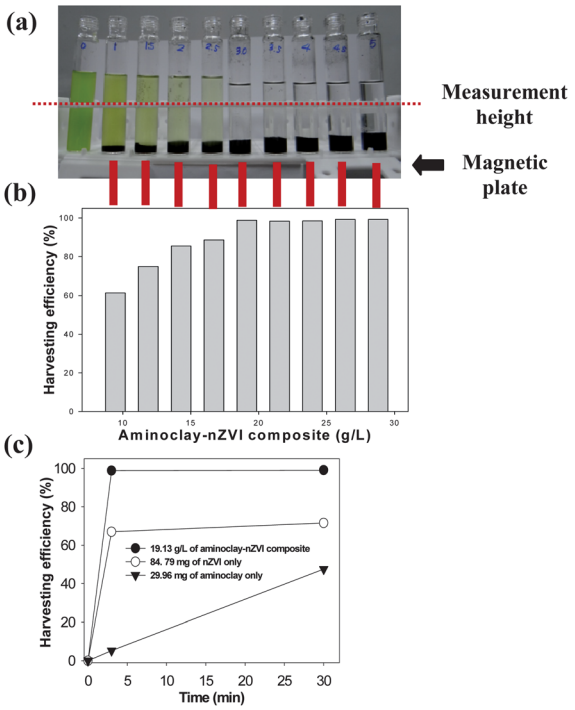

Fig. 4 Microalgae harvesting kinetics. Dica photograph (a) and its corresponding harvesting efficiencies (%) (b), and kinetics of bare nZVI and only-aminoclay based on 19.13 g L^{-1} of aminoclay–nZVI composite (c).

Fig. S9 and Movie S1†). This is a very fast reaction, comparable to the previously reported results.[11,12] For this loading range, the harvesting efficiencies attained were ~100% (see ESI, Fig. S10†). To investigate the effect of only-aminoclay (29.96 mg) and pure nZVI (84.79 mg), the concentrations of them were calculated based on 19.13 g L^{-1} of aminoclay–nZVI composite, microalgae harvesting experiments were performed. The harvesting efficiencies by only-aminoclay were ~65% at 3 min and ~70% at 30 min, while those of pure nZVI were ~5% at 3 min and ~40% at 30 min (Fig. 4c). It is imperative that aminoclay-coated nZVI shows a synergic harvesting efficiency from the viewpoint of both efficiency and time for equivalent amounts. The mechanism of efficient harvesting by aminoclay–nZVI composites is attributed mainly to the cationic property of aminoclay and induction of magnetic force from nZVI. The morphologies of the microalgae harvested by aminoclay–nZVI were shown to be intact, as confirmed by chlorophyll-emitting red fluorescence and SEM images (see ESI, Fig. S11†), meaning that cell effects by radical generation of nZVI was negligible,[44] Notably, the pH was changed from 6.2 to ~9.0 in most cases (see ESI, Fig. S12†); this was due to the aminoclay's protonated amine groups and nZVI's marginal production of H_2 where the aminoclay coating covered the nZVI surface by non-covalent bonding.

Feasibility study of scaled-up (24 L) microalgae harvesting process with aminoclay–nZVI composite (ratio 1.0)

For practical application of this composite, a scaled-up process is required.[1–3,10] To that end, a rectangular reactor (50 cm × 12 cm × 40 cm) was designed (see the Fig. S13† scheme). Flocculated microalgae biomass was collected on the surfaces of magnetic rods inserted into microalgal solution or precipitated for 15 min to facilitate harvesting (see ESI, Fig. S14 and Movie S2†). After finishing harvesting, some aminoclay was released (<0.2 g L^{-1}), nZVI oxidation proceeded slowly. However, it is anticipated that this process, due to its recyclability, could be applied on the tone scale in the continuous mode where integration system is consisted of parallel-based many 20 L tubes. The aminoclay–nZVI composite could easily be separated by acid digestion from a collected biomass,[11] and recovered by Fe^{3+} reduction by polyphenols,[45] given that it is considered initial investment cost of magnetic nanoparticle. From now on, optimization of the container, magnetic rods, and mixing techniques is additionally required. Currently, we are planning lipid extraction from wet-microalgal biomasses using Fenton-like reaction with injection of hydrogen peroxide (H_2O_2).[29]

Conclusions

In summary, the characteristic time (τ) and hydrodynamic diameter of aggregates of aminoclay-coated nZVI composites were evaluated as functions of sedimentation rate. The results showed that the optimal stability was achieved at the 1.0 aminoclay–nZVI ratio, which effected the smallest aggregate size (~100 nm) and a highly positively charged surface. Using the aminoclay–nZVI composite at the ratio (1.0) in which aminoclay uniformly coated the nZVI nanoparticles, oleaginous microalgae harvesting was successfully demonstrated. Within 3 min, ~100% of *Chlorella* sp. KR-1 was harvested at a > 20 g L^{-1} loading of aminoclay–nZVI composite under an external magnetic field. A scaled-up (24 L) harvesting process entailing microalgae collection on the surfaces of introduced magnetic rods or by precipitation was successfully conducted. It is believed that this novel strategy, due to the recyclability of aminoclay–nZVI composite and the reduction of aminoclay amount thereby enabled, can be effectively and efficiently applied to continuous harvesting.

Acknowledgements

This work was supported by the Advanced Biomass R&D Center (ABC) of the Global Frontier Project funded by the Ministry of Education, Science and Technology (ABC-2012-053880), by the Korea Institute of Energy Technology Evaluation and Planning (KETEP) and the Korean Ministry of Knowledge Economy (MKE) as part of the Energy Efficiency and Resources R&D project "Process demonstration for bioconversion of CO_2 to high-valued biomaterials using microalgae" (2012-T-100201516), and by a grant from the New & Renewable Energy Technology Development Program of the Korea Institute of Energy Technology Evaluation and Planning (KETEP) funded by the Korean Ministry of Knowledge Economy (no. 20123010090010). We thank Jin Seok Choi of the KAIST Research Analysis Center for the TEM imaging and its analysis. Yuhoon Hwang acknowledges funding for this study through an H. C. Ørsted Postdoc Program stipend from Technical University of Denmark (DTU).

Henrik R. Andersen received funding from DTU for this work through a strategic research initiative in co-operation with KAIST.

Notes and references

1 R. H. Wijffels and M. J. Barbosa, *Science*, 2010, **329**, 796.
2 R. H. Wijffels, M. J. Barbosa and M. H. M. Eppink, *Biofuels, Bioprod. Biorefin.*, 2010, **4**, 287.
3 R. Luque, L. Herrero-Davila, J. M. Campelo, J. H. Clark, J. M. Hidalgo, D. Luna, J. M. Marinas and A. A. Romero, *Energy Environ. Sci.*, 2008, **1**, 542.
4 Y. C. Sharma, B. Singh and J. Korstad, *Green Chem.*, 2011, **13**, 2993.
5 S. Zou, Y. Wu, M. Yang, C. Li and J. Tong, *Energy Environ. Sci.*, 2010, **3**, 1073.
6 F. Shi, P. Wang, Y. Duan, D. Link and B. Morreale, *RSC Adv.*, 2012, **2**, 9727.
7 J. Kim, G. Yoo, H. Lee, J. Lim, K. Kim, C. W. Kim, M. S. Park and J.-W. Yang, *Biotechnol. Adv.*, 2013, **31**, 862.
8 D.-G. Kim, H.-J. La, C.-Y. Ahn, Y.-H. Park and H.-M. Oh, *Bioresour. Technol.*, 2011, **102**, 3163.
9 C.-Y. Chen, K.-L. Yeh, R. Aisyah, D.-J. Lee and J.-S. Chang, *Bioresour. Technol.*, 2011, **102**, 71.
10 W. Farooq, Y.-C. Lee, J.-I. Han, C. H. Darpito, M. Choi and J.-W. Yang, *Green Chem.*, 2013, **15**, 749.
11 L. Xu, C. Guo, F. Wang, S. Zheng and C.-Z. Liu, *Bioresour. Technol.*, 2011, **102**, 10047.
12 Y.-R. Hu, F. Wang, S.-K. Wang, C.-Z. Liu and C. Guo, *Bioresour. Technol.*, 2013, **138**, 387.
13 K. Lee, S. Y. Lee, J.-G. Na, S. G. Jeon, R. Praveenkumar, D.-M. Kim, W.-S. Chang and Y.-K. Oh, *Bioresour. Technol.*, 2014, **149**, 575.
14 S. Mann, S. L. Burkett, S. A. Davis, C. E. Fowler, N. H. Mendelson, S. D. Sims, D. Walsh and N. T. Whilton, *Chem. Mater.*, 1997, **9**, 2300.
15 S. Mann, *Nat. Mater.*, 2009, **8**, 781.
16 K. K. R. Datta, A. Achari and M. Eswaramoorthy, *J. Mater. Chem. A*, 2013, **1**, 6707.
17 A. J. Patil and S. Mann, *J. Mater. Chem.*, 2008, **18**, 4605.
18 J. L. Vickery, S. Thachepan, A. J. Patil and S. Mann, *Mol. BioSyst.*, 2009, **5**, 744.
19 S. C. Holmström, A. J. Patil, M. Butler and S. Mann, *J. Mater. Chem.*, 2007, **17**, 3894.
20 P. Chaturbedy, D. Jagadeesan and M. Eswaramoorthy, *ACS Nano*, 2010, **4**, 5921.
21 Y.-C. Lee, E. J. Kim, D. A. Ko and J.-W. Yang, *J. Hazard. Mater.*, 2011, **196**, 101.
22 Y.-C. Lee, E. J. Kim, J.-W. Yang and H.-J. Shin, *J. Hazard. Mater.*, 2011, **192**, 62.
23 Y.-C. Lee, E. J. Kim, H.-J. Shin, M. Choi and J.-W. Yang, *J. Ind. Eng. Chem.*, 2012, **18**, 871.
24 Y.-C. Lee, S.-J. Chang, M.-H. Choi, T.-J. Jeon, T. Ryu and Y. S. Huh, *Appl. Catal., B*, 2013, **142–143**, 494.
25 Y.-C. Lee, Y.-S. Choi, M. Choi, H. Yang, K. Liu and H.-J. Shin, *Appl. Clay Sci.*, 2013, **83–84**, 474.
26 Y.-C. Lee, E. Jin, S. W. Jung, Y.-M. Kim, K. S. Chang, J.-W. Yang, S.-W. Kim, Y.-O. Kim and H.-J. Shin, *Sci. Rep.*, 2013, **3**, 1292.
27 Y.-C. Lee, B. Kim, W. Farooq, J. Chung, J.-I. Han, H.-J. Shin, S. H. Jeong, J.-Y. Park, J.-S. Lee and Y.-K. Oh, *Bioresour. Technol.*, 2013, **132**, 440.
28 Y.-C. Lee, Y. S. Huh, W. Farooq, J. Chung, J.-I. Han, H.-J. Shin, S. H. Jeong, J.-S. Lee, Y.-K. Oh and J.-Y. Park, *Bioresour. Technol.*, 2013, **137**, 74.
29 Y.-C. Lee, Y. S. Huh, W. Farooq, J.-I. Han, Y.-K. Oh and J.-Y. Park, *RSC Adv.*, 2013, **3**, 12802.
30 W.-X. Zhang, *J. Nanopart. Res.*, 2003, **5**, 323.
31 P. G. Tratnyek and R. L. Johnson, *Nano Today*, 2006, **1**, 44.
32 K. K. R. Datta, G. Kulkarni and M. Eswaramoorthy, *Chem. Commun.*, 2010, **46**, 616.
33 J. Guo, R. Wang, W. W. Tjiu, J. Pan and T. Liu, *J. Hazard. Mater.*, 2012, **225–226**, 63.
34 M. Breulmann, H. Cölfen, H.-P. Hentze, M. Antonietti, D. Walsh and S. Mann, *Adv. Mater.*, 1998, **10**, 237.
35 Y. Hwang, D.-G. Kim and H.-S. Shin, *Appl. Catal., B*, 2011, **105**, 144.
36 T. Phenrat, N. Saleh, K. Sirk, R. D. Tilton and G. V. Lowry, *Environ. Sci. Technol.*, 2007, **41**, 284.
37 A. Tiraferri, K. L. Chen, R. Sethi and M. Elimelech, *J. Colloid Interface Sci.*, 2008, **324**, 71.
38 G. C. C. Yang, H.-C. Tu and C.-H. Hung, *Sep. Purif. Technol.*, 2007, **58**, 166.
39 Y. Hwang, Y.-C. Lee, P. D. Mines, Y. S. Huh and H. R. Andersen, *Appl. Catal., B*, 2014, **147**, 748.
40 Y.-C. Lee, C.-W. Kim, J.-Y. Lee, H.-J. Shin and J.-W. Yang, *Desalin. Water Treat.*, 2009, **10**, 33.
41 J. Shin, Y.-C. Lee, Y. Ahn and J.-W. Yang, *Desalin. Water Treat.*, 2012, **50**, 102.
42 H. Niu, Y. Wang, X. Zhang, Z. Meng and Y. Cai, *ACS Appl. Mater. Interfaces*, 2012, **4**, 286.
43 F. Mou, j. Guan, H. Ma, L. Xu and W. Shi, *ACS Appl. Mater. Interfaces*, 2012, **4**, 3987.
44 B. Marsalek, D. Jancula, E. Marsalkova, M. Mashlan, K. Safarova, J. Tucek and R. Zboril, *Environ. Sci. Technol.*, 2012, **46**, 2316.
45 G. E. Hoag, J. B. Collins, J. L. Holcomb, J. R. Hoag, M. N. Nadagouda and R. S. Varma, *J. Mater. Chem.*, 2009, **19**, 8671.